

This discussion paper is/has been under review for the journal Hydrology and Earth System Sciences (HESS). Please refer to the corresponding final paper in HESS if available.

# Estimate soil moisture using trapezoidal relationship between remotely sensed land surface temperature and vegetation index

W. Wang, D. Huang, X.-G. Wang, Y.-R. Liu, and F. Zhou

State Key Laboratory of Hydrology-Water Resources and Hydraulic Engineering,  
Hohai University, Nanjing, 210098, China

Received: 26 October 2010 – Accepted: 26 October 2010 – Published: 3 November 2010

Correspondence to: W. Wang (w.wang@126.com)

Published by Copernicus Publications on behalf of the European Geosciences Union.

8703

## Abstract

The trapezoidal relationship between surface temperature ( $T_s$ ) and vegetation index (VI) was used to estimate soil moisture in the present study. An iterative algorithm is proposed to estimate the vertices of the  $T_s \sim VI$  trapezoid theoretically for each grid, and then WDI is calculated for each grid using MODIS remotely sensed measurements of surface temperature and enhanced vegetation index (EVI). The capability of using WDI based on  $T_s \sim VI$  trapezoid to estimate soil moisture is evaluated using soil moisture observations and antecedent precipitation in the Walnut Gulch Experimental Watershed (WGEW) in Arizona, USA. The result shows that,  $T_s \sim VI$  trapezoid based WDI can well capture temporal variation in surface soil moisture, but the capability of detecting spatial variation is poor for such a semi-arid region as WGEW.

## 1 Introduction

In 1980s', it was found that, land surface temperature ( $T_s$ ) and the fraction of vegetation cover, which is represented by vegetation indices (e.g., NDVI), typically show a strong negative relationship (e.g., Goward et al., 1985; Nemani and Running, 1989). Such a relationship has been widely used to investigate the moisture condition of land surfaces. Several studies focused on the slope of the  $T_s$ /NDVI curve for providing information on vegetation and moisture conditions at the surface (e.g., Smith and Choudhury, 1991; Nemani et al., 1993). Their approach was later extended to use the information in the  $T_s$ /VI scatter-plot space, whose envelope is considered to be in either a triangular shape (e.g., Price, 1990; Carlson et al., 1994), or a trapezoid shape (e.g., Moran et al., 1994).

The idea of triangle  $T_s$ /VI space has been used to develop the so called “triangle method”, and has been applied by a lot of researchers (e.g., Gillies et al., 1997; Sandholt et al., 2002; Margulis et al., 2005; Tang et al., 2010). The “triangle” method fits the scatter-plot of observed vegetation index (VI) and land surface temperature ( $T_s$ ) using

8704

a triangle. The central assumption of the triangle method is that, given a large number of pixels reflecting a full range of soil surface wetness and fractional vegetation cover, sharp boundaries (edges) in the data reflect real physical limits: i.e., bare soil, 100% vegetation cover, and lower and upper limits of the surface soil water content, e.g., completely dry or wet (field capacity), respectively. The dry and wet edges ultimately intersect at a (truncated) point at full vegetation cover. Then, based on the triangle, the relative value of surface soil water content and the surface energy fluxes at each pixel can be defined in terms of its position within the triangle. The advantage of the triangle method is its independence of ancillary data. The approach, however, has difficulty in defining the dry and wet edge, especially the dry edge. Even with a large number of remotely sensed observations, the boundaries of the triangle space are still hard to be well established, because on one hand, there are situations when  $VI-T_s$  points scatter in a close range such as during rainy season or in areas with a narrow VI range; on the other hand, the  $T_s \sim VI$  relationship is much more complicated at large scale than at local scale and may vary at different parts due to heterogeneity in land surface properties and atmospheric forcing. Furthermore, because the triangle space is established empirically, the soil moisture estimates according to such an empirical triangle using an image at one time are hard to be compared with those at another time.

Moran et al. (1994) proposed the idea of vegetation index/temperature (VIT) trapezoid, and the water deficit index (WDI) for evaluating evapotranspiration rates of both full-cover and partially vegetated sites. However, very few applications were found in the literature based on the idea of trapezoid  $T_s/VI$  space for estimating soil moisture. In the present paper, we will extend the idea of VIT trapezoid and WDI, for estimating soil moisture estimation using MODIS products. The method, referred to as the trapezoid method, will be described in detail in Sect. 2. Then the method will be applied to the Walnut Gulch Experimental Watershed in Arizona, USA, for which, the data used and data pre-process will be introduced in Sects. 3 and 4, and the results will be presented in Sect. 5. Finally, some conclusions will be drawn in Sect. 6.

8705

## 2 Trapezoid method

### 2.1 The concept of $(T_s - T_a) \sim V_c$ trapezoid

Idso et al. (1981) and Jackson et al. (1981) proposed the CWSI (Crop Water Stress Index) for detecting plant water stress based on the difference between canopy and air temperature. It is designed for full-cover vegetated areas and bare soils at local and regional scales. To overcome the difficulty of measuring foliage temperature in partially vegetated fields, Moran et al. (1994) proposed to use the shape of trapezoid to depict the relationship between the surface temperature and air temperature difference ( $T_s - T_a$ ) vs. the fractional vegetation cover ( $V_c$ , ranging from 0 for bare soil to 1 for full-cover vegetation) (Fig. 1), so as to combine spectral vegetation indices with composite surface temperature measurements to allow application of the CWSI theory to partially vegetated fields without a priori knowledge of the percent vegetation cover. Based on the trapezoid assumption and the CWSI theory, Moran et al. (1994) introduced the Water Deficit Index (WDI) for evaluating field evapotranspiration rates and relative field water deficit for both full-cover and partially vegetated sites. For a given pixel with measured surface temperature and air temperature difference, i.e.,  $(T_s - T_a)_r$ , WDI is defined as:

$$WDI = \frac{(T_s - T_a)_{\min} - (T_s - T_a)_r}{(T_s - T_a)_{\min} - (T_s - T_a)_{\max}} \quad (1)$$

where  $T_a$  is air temperature;  $T_s$  is surface temperature; the subscripts min, max, and r refer to minimum, maximum, and measured values, respectively; and the minimum and maximum values of  $(T_s - T_a)$  are interpolated linearly on the cold edge and warm edge of the  $(T_s - T_a) \sim V_c$  trapezoid for the specific  $V_c$  value of the pixel. Graphically, WDI is equal to the ratio of distances AC/AB in Fig. 1.

8706













The strips in Band 5 data mostly are lines of one pixel in width, which are distinguishable from neighbouring pixels. To identify the strips, we firstly define the following two convolution kernels:

$$k_1 = \begin{bmatrix} 0 & -1 & 0 \\ 0 & 1 & 0 \\ 0 & 0 & 0 \end{bmatrix} \quad k_2 = \begin{bmatrix} 0 & 0 & 0 \\ 0 & 1 & 0 \\ 0 & -1 & 0 \end{bmatrix}$$

5 Then, we calculate  $KK = \text{convol}(D, k_1) \times \text{convol}(D, k_2)$ , where  $\text{convol}(\bullet)$  is the convolution filtering function in IDL, and  $D$  is the data to be processed. A pixel in a strip is identified if  $KK > 0.001$  for this pixel. For bad pixels, linear interpolation is applied to replace the bad values using the values of upside and downside neighboring pixels.

Besides the strips of one pixel width, there are also some strips with two pixels in width resulted from the process of projection conversion in Band 5 of MOD09A1 albedo product. Considering that the pixels in strips have normally higher values than normal, we identify pixels with values larger than 0.35 as “bad” pixels. Then we interpolate the bad pixels with neighbouring “good” pixels with the method of Delaunay triangle (using the program DEM\_BAD\_DATA\_DOIT in IDL). In the same way, pixels with value of 0 are also treated.

15 With the above two procedures, the quality of Band 5 albedo product was significantly improved (see Fig. 5).

## 4.2 Denosing the MOD13A1 vegetation index data

When observing the land surface, MODIS is inevitably impacted by the variation of satellite orbital position, cloud coverage and other atmospheric effects. Although several methods (such as Maximum Value Composites or Constrained View Maximum Value Composite) have been applied to reduce the noise impacts the MODIS NDVI/EVI products, quite amount of noise still exist in the VI dataset, and filtering is still necessary when using them for constructing  $T_s \sim VI$  space.

8717

Many methods are available to denoise the MODIS NDVI/EVI data. Jennifer (2009) compared several methods, and found that the asymmetric Gaussian, Double logistic, and 4253H twice filter perform very well in general. Therefore, one of them, i.e., 4253H twice filter (Velleman, 1980) was adopted here. The 4253H twice filter applies a series of running medians of varying window size and a weighted average filter (e.g., Hanning filter), with re-roughing, to the EVI time series.

To perform the denoising process, a series of continuous EVI data over one year are required. Therefore, before we use the MODIS data selected for 10 dates, we used 25 consecutive 16-day composite EVI data (the last 16-day composite data in 2003, all 23 16-day composite EVI data in 2004, together with the first 16-day composite data in 2005) to conduct the denoising procedure. The effects of denoising for two randomly selected pixels are shown in Fig. 6, from which we see that, both low values and high values are smoothed.

## 4.3 Topographic correction of air temperature

15 With methods of estimating soil moisture using thermal satellite images, often both land surface temperature and ground-based air temperature observations are needed. When applying such methods to mountainous regions, terrain effects have to be taken into account because terrain would significantly affect both land surface temperature and air temperature. To avoid the problem of steeply sloping terrain, some authors just eliminated those pixels in mountainous part (e.g., Carlson et al., 1994), while in some other cases, land surface temperature was corrected (e.g., Hassan et al., 2007). In the present study, we go the opposite way, i.e., instead of correct land surface temperature, we correct the air temperature.

20 To make a successful air temperature interpolation, many factors should be taken into account, such as the difference in elevation between grid points and monitoring stations, temperature vertical gradient, geometric characteristics (slope, aspect) of each grid cell, and vegetation coverage. Moore et al. (1993) proposed a specific algorithm

8718









- Idso, S. B., Aase, J. K., and Jackson, R. D.: Net radiation – Soil heat flux relations as influenced by soil water content variations, *Bound.-Lay. Meteorol.*, 9, 113–122, 1975.
- Idso, S. B., Jackson, R. D., Pinter Jr., P. J., Reginato, R. J., and Hatfield, J. L.: Normalizing the stress-degree-day parameter for environmental variability, *Agr. Meteorol.*, 24, 45–55, 1981.
- 5 Iziomon, M. G., Mayer, H., and Matzarakis, A.: Downward atmospheric longwave irradiance under clear and cloudy skies: Measurement and parameterization, *J. Atmos. Sol.-Terr. Phy.*, 65, 1107–1116, 2003.
- Jackson, R. D., Idso, S. B., Reginato, R. J., and Pinter, P. J.: Canopy temperature as a crop water stress indicator, *Water Resour. Res.*, 17, 1133–1138, 1981.
- 10 Jennifer, N. H. and McDermid, G. J.: Noise reduction of NDVI time series: An empirical comparison of selected techniques, *Remote Sens. Environ.*, 113, 248–258, 2009.
- Kustas, W. P., Choudhury, B. J., Moran, M. S., Reginato, R. J., Jackson, R. D., Gay, L. W., and Weaver, H. L.: Determination of sensible heat flux over sparse canopy using thermal infrared data, *Agr Forest Meteorol.*, 44, 197–216, 1989.
- 15 Liang, S.: Retrieval of Land Surface Albedo from Satellite Observations: A Simulation Study[J], *J. Appl. Meteorol.*, 38, 712–725, 1999.
- Margulis, S. A., Kim, J., and Hogue, T.: A Comparison of the Triangle Retrieval and Variational Data Assimilation Methods for Surface Turbulent Flux Estimation, *J. Hydrometeorol.*, 6, 1063–1072, 2005.
- 20 McCutchan, M. H. and Fox, D. G.: Effect of Elevation and Aspect on Wind, Temperature and Humidity, *J. Clim. Appl. Meteorol.*, 25(12), 1996–2013, 1986.
- Moran, M. S., Clarke, T. R., Inoue, Y., and Vidal, A.: Estimating crop water deficit using the relation between surface air temperature and spectral vegetation index, *Remote Sens. Environ.*, 49, 246–263, 1994.
- 25 Nemani, R. R. and Running, S. W.: Estimation of regional surface resistance to evapotranspiration from NDVI and thermal IR AVHRR data, *J. Appl. Meteorol.*, 28, 276–284, 1989.
- Nemani, R. R., Pierce, L., Running, S. W., and Goward, S.: Developing satellite-derived estimates of surface moisture status, *J. Appl. Meteorol.*, 32, 548–557, 1993.
- Pellenq, J., Kalma, J., Boulet, G., Saulnier, G. M., Wooldridge, S., Kerr, Y., and Chehbouni, A.:  
30 A disaggregation scheme for soil moisture based on topography and soil depth, *J. Hydrol.*, 276, 112–127, 2003.
- Price, J. C.: Using spatial context in satellite data to infer regional scale evapotranspiration [J], *IEEE T. Geosci. Remote*, 28, 940–948, 1990.

8725

- Renard, K. G., Lane, L. J., Simanton, J. R., Emmerich, W. E., Stone, J. J., Weltz, M. A., Goodrich, D. C., and Yakowitz, D. S.: Agricultural impacts in an arid environment: Walnut Gulch case study, *Hydrol. Sci. Tech.*, 9(1–4), 145–190, 1993.
- 5 Sandholt, I., Rasmussen, K., and Andersen, J.: A Simple Interpretation of the Surface Temperature/Vegetation Index Space for Assessment of Surface Moisture Status, *Remote Sens. Environ.*, 79(2), 213–224, 2002 .
- Scurlock, J. M. O., Asner, G. P., and Gower, S. T.: Global Leaf Area Index Data from Field Measurements, 1932–2000, Data set, available on-line at <http://www.daac.ornl.gov> from the Oak Ridge National Laboratory Distributed Active Archive Center, last access: 1 August 2010, Oak Ridge, Tennessee, USA, 2001.
- 10 Shuttleworth, W. and Wallace, J.: Evaporation from Sparse Crops – An Energy Combination Theory, *Q. J. Roy. Meteor. Soc.*, 111, 839–855, 1985.
- Skirvin, S., Kidwell, M., Biedenbender, S., Henley, J. P., King, D., Collins, C. H., Moran, S., and Weltz, M.: Vegetation data, Walnut Gulch Experimental Watershed, Arizona, United States,  
15 *Water Resour. Res.*, 44, W05S08, doi:10.1029/2006WR005724, 2008.
- Smith, R. C. G. and Choudhury, B. J.: Analysis of normalized difference and surface temperature observations over southeastern Australia, *Int. J. Remote Sens.*, 12(10), 2021–2044, 1991.
- 20 Tang, R., Li, Z.-L., and Tang, B.: An application of the  $T_sVI$  triangle method with enhanced edges determination for evapotranspiration estimation from MODIS data in arid and semi-arid regions: Implementation and validation, *Remote Sens. Environ.*, 114, 540–551, 2010.
- Velleman, P.: Definition and comparison of robust nonlinear data smoothing algorithms, *J. Am. Stat. Assoc.*, 75, 609–615, 1980.
- World Meteorological Organization (WMO): Guide to Meteorological Instruments and Methods of Observation, WMO-No. 8 (CIMO Guide), Geneva, 2008.
- 25 Zillman, J. W.: A study of some aspects of the radiation and heat budgets of the southern hemisphere oceans, Canberra: Australian Government Publishing Service, Canberra, Australia, 1972.

8726



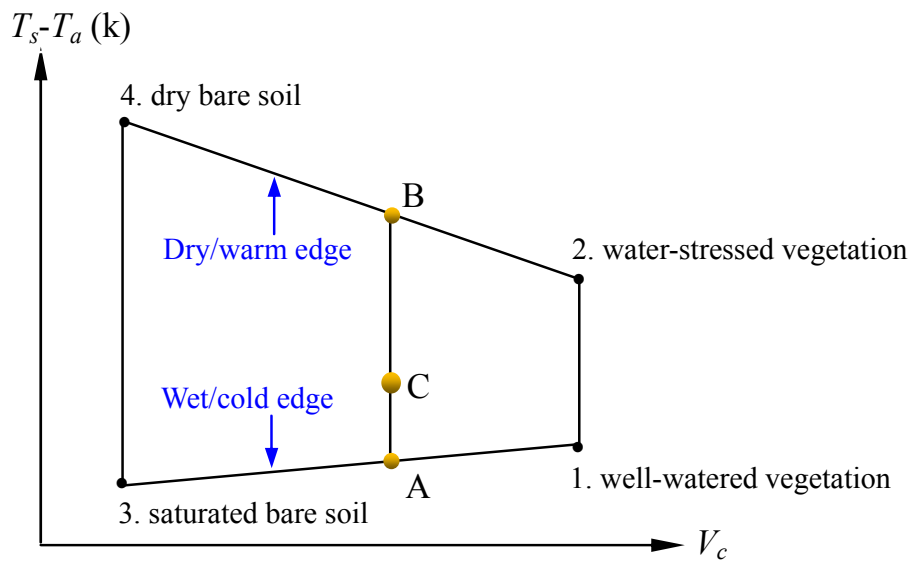


**Fig. 1.** The hypothetical trapezoidal shape based on the relation between  $(T_s - T_a)$  and the fractional vegetation cover ( $V_c$ ).

8729

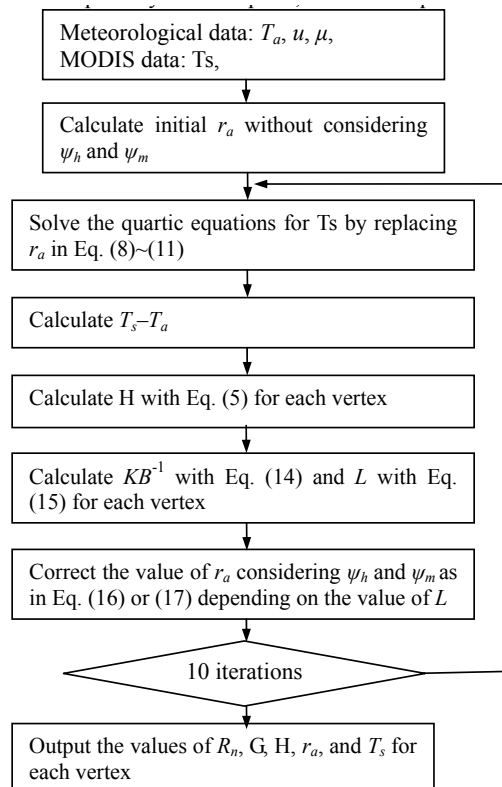


**Fig. 2.** Iterative procedure for calculating  $T_s$  of the four vertices of  $T_s$ -VI trapezoid.

8730



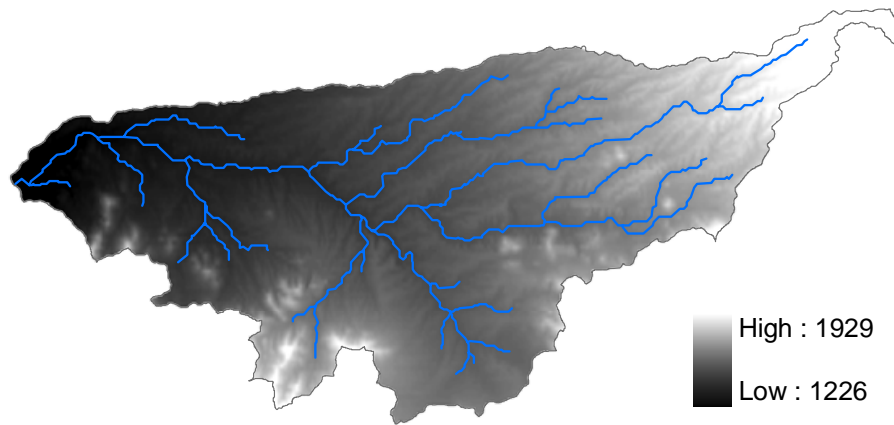


Fig. 3. Digital elevation model (DEM) of Walnut Gulch Experimental.

8731

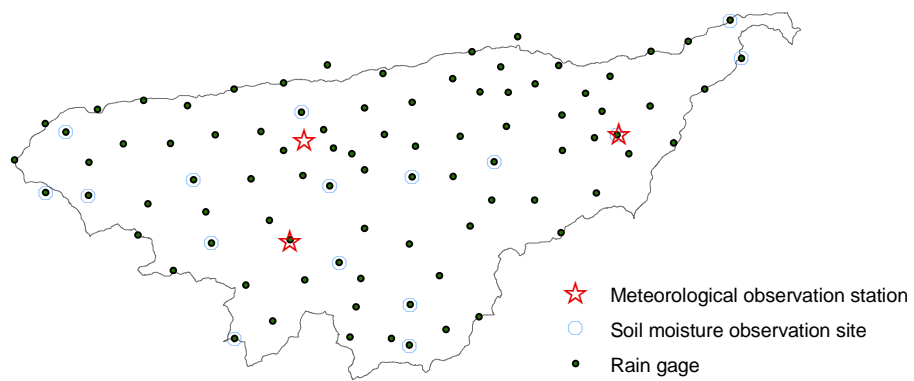
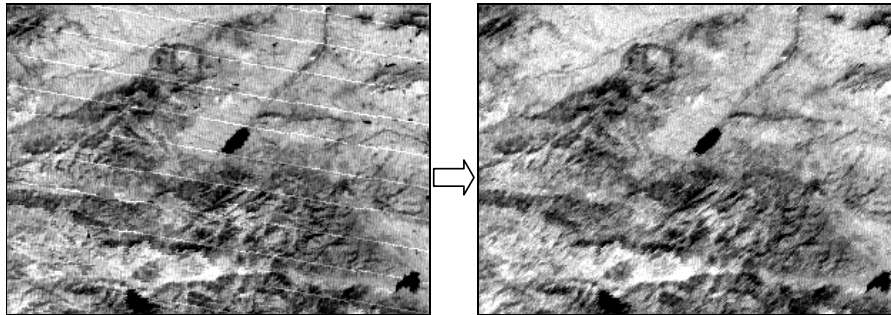


Fig. 4. Locations of ground-based observation sites in WGEW.

8732



**Fig. 5.** Comparison of Band 5 albedo images before (left) and after destriping.

8733

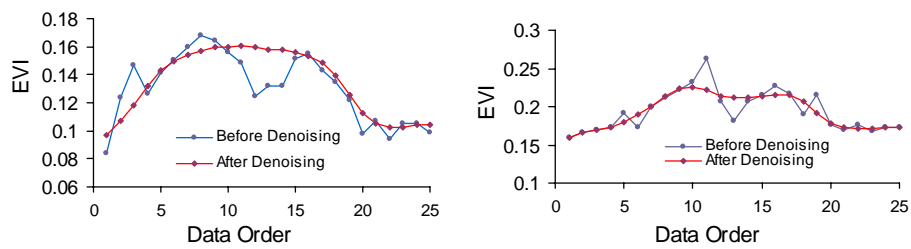


**Fig. 6.** Effects of EVI denoising preprocessing for two randomly selected pixels.

8734

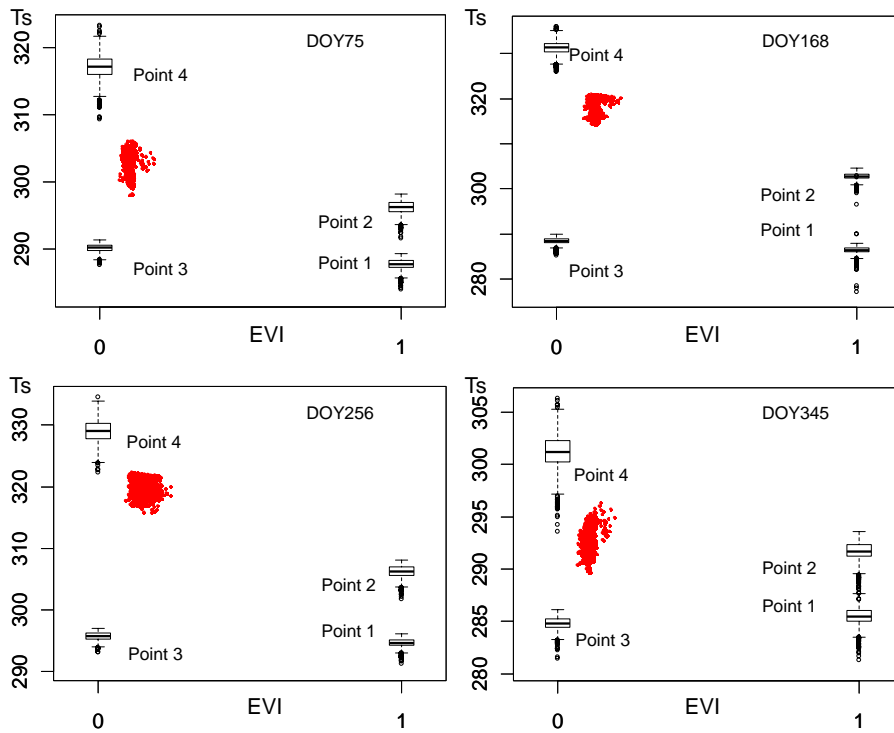


**Fig. 7.** Constructed  $T_s$ -EVI trapezoids in four dates in four different seasons.

8735

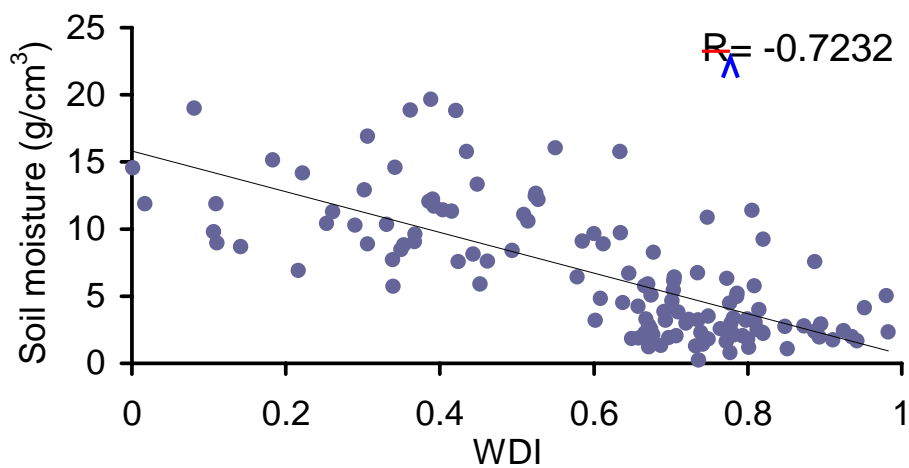


**Fig. 8.** WDI estimates vs. ground observations at 16 sites in 10 dates ( $R$  is the correlation coefficient).

8736

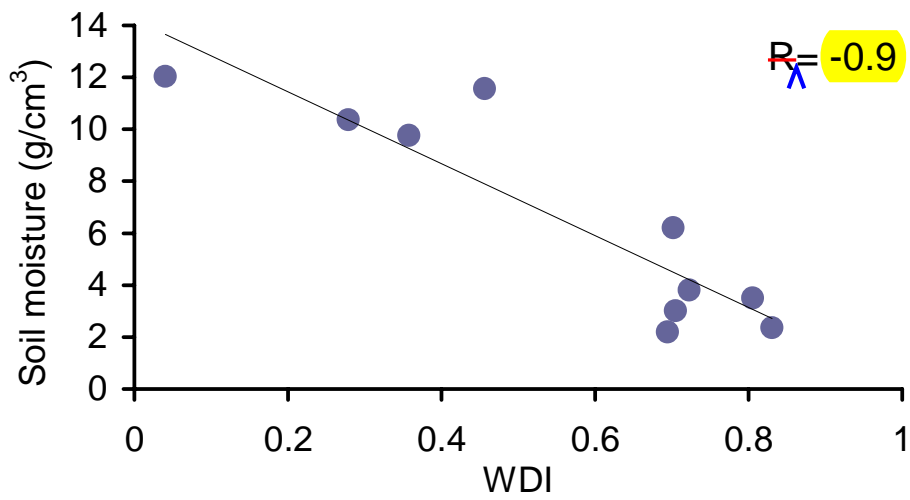


**Fig. 9.** The average WDI estimates vs. the average ground observations in 10 dates ( $R$  is the correlation coefficient).

8737

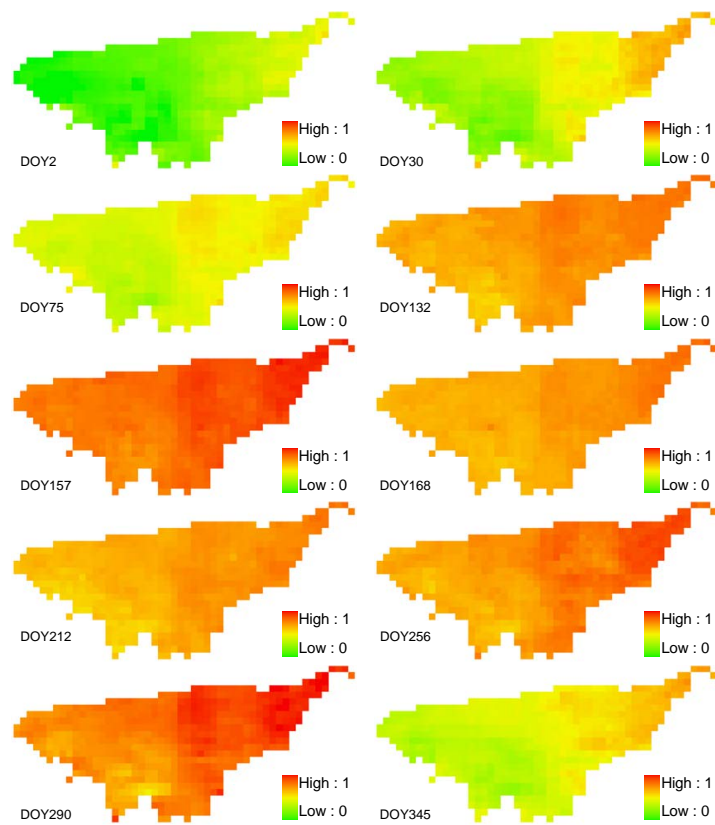


**Fig. 10.** WDI maps for 10 DOYs.

8738

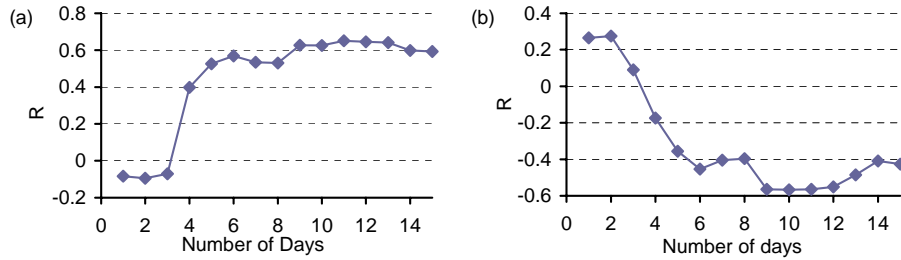


**Fig. 11.** Correlation coefficient ( $R_{\lambda}$ ) between (a) soil moisture observation and AP of different number of days, and (b) WDI and AP of different number of days.

8739

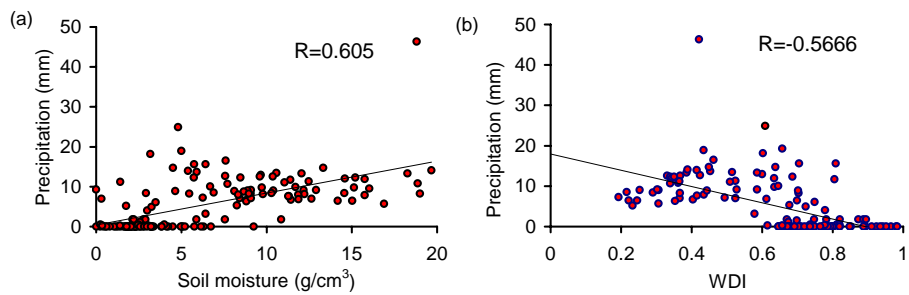


**Fig. 12.** Scatter plot of (a) soil moisture observation and (b) WDI vs. 10-day AP ( $R_{\lambda}$  is the coefficient of correlation).

8740